Rice Hull Biocomposites. I. Preparation of a Linseed-Oil-Based Resin Reinforced with Rice Hulls

Rafael L. Quirino, Richard C. Larock

Department of Chemistry, Iowa State University, 2751 Gilman Hall, Ames, Iowa 50011

Received 18 June 2010; accepted 20 October 2010
DOI 10.1002/app.33630
Published online 16 March 2011 in Wiley Online Library (wileyonlinelibrary.com).

ABSTRACT: Biocomposites consisting of a conjugated linseed-oil (CLO)-based thermoset reinforced with rice hulls were prepared by free-radical polymerization initiated by *t*-butyl peroxide. The resin composition was kept constant at 50 wt % CLO, 35 wt % *n*-butyl methacrylate, and 15 wt % divinylbenzene. Tensile tests, dynamic mechanical analysis, thermogravimetric analysis, Soxhlet extraction, and differential scanning calorimetry were used to establish the ideal cure sequence. The pressure during cure, filler load, and the drying and grinding of the filler were varied, and their effects on the final properties of the composites were assessed. Optimal conditions were established for the preparation of rice hull biocomposites. Scanning electron microscopy showed a weak filler–resin interaction and X-ray mapping suggested the presence of silica in the rice hulls; this have accounted for the high thermal and mechanical properties obtained for these composites. © 2011 Wiley Periodicals, Inc. J Appl Polym Sci 121: 2039–2049, 2011

Key words: biomaterials; composites; copolymerization

INTRODUCTION

The rapid increase in petroleum prices over recent years has encouraged the development of alternative sources of energy and materials. In that context, biorenewable-based products, such as biofuels, bioplastics, and biocoatings are especially appealing because they are readily prepared from naturally occurring starting materials that are constantly being generated by nature. Although the complete substitution of petroleum-derived products in our current society is highly unlikely, great progress has been made recently toward the development of products with the potential to compete with petroleum goods in times of high oil prices.

With that in mind, our group has investigated the synthesis and properties of new biomaterials derived mainly from agricultural oils. Materials, such as soybean oil-based polyurethane coatings,[1,2] soybean-[3,4] and linseed-oil-based biorubbers,[5] and various bioplastics containing at least 40 wt % vegetable or modified vegetable oils, such as soybean,[6] corn,[7] tung,[8] and linseed oils,[9] have been prepared and analyzed. These latter materials range from soft rubbers to hard plastics, depending on the resin composition and the comonomers added to the matrix.[10]

Correspondence to: R. C. Larock (larock@iastate.edu).
Contract grant sponsor: Recycling and Reuse Technology Transfer Center of the University of Northern Iowa.

The use of natural fibers to reinforce polymeric materials has been explored by several groups in the last decade. There have been reports on the reinforcement of polypropylene with sisal fiber,[11] rice hulls and kenaf fiber,[12] palm and coir fibers,[13] wheat straw,[14] sunflower hulls,[15] and abaca strands.[16] High density polyethylene has also been reinforced with banana fiber,[17] sugar cane bagasse, and wood flour.[18] Polyester and epoxy resin have been reinforced with jute fiber,[19] and there have been reports on the use of hemp fiber[20] and poultry feathers as reinforcements for composites,[21] among several other combinations of resin and natural fibers that are not cited here.

Recently, our group reported on the preparation and analysis of a soybean oil-based thermoset resin reinforced with corn stover.[22] We previously reinforced the same resin with soybean hulls,[23] and a tung-oil variation of the resin was reinforced with spent germ.[24,25] Unlike in the previous study, where rice hulls were used to reinforce thermoplastics,[12] we report herein the preparation of a linseed oil-based free-radical thermoset resin reinforced with rice hulls. The resin was a copolymer of conjugated linseed oil (CLO), divinylbenzene (DVB), and *n*-butyl methacrylate (BMA). The composites were compression molded, and the influence of pressure during cure, cure temperatures, cure time, filler load, filler particle size, and drying of the filler on the final properties of the composites was assessed, and the optimum preparation conditions are proposed. The techniques used for the analysis of the biocomposites were tensile tests, dynamic mechanical analysis (DMA), differential

TABLE I
Cure Temperatures Used in the Preparation of the Biocomposites

Cure sequence[a]	Cure temperature (°C)	Postcure temperature (°C)
I	130	150
II	140	160
III	155	175
IV	180	200
V	230	250
VI	180	–
VII	180[b]	–

[a] The composites were cured under 400 psi.
[b] The sample was cured for 7 h.

scanning calorimetry (DSC), thermogravimetric analysis (TGA), Soxhlet extraction, proton nuclear magnetic resonance spectroscopy (^{1}H-NMR), scanning electron microscopy (SEM), and X-ray mapping.

EXPERIMENTAL

Materials

BMA was purchased from Alfa Aesar (Ward Hill, MA). DVB and *t*-butyl peroxide were purchased from Sigma-Aldrich (Milwaukee, WI). All were used as received. Superb linseed oil was provided by ADM (Red Wing, MN) and was conjugated with a rhodium catalyst by a method developed and frequently used by our group.[26] The rice hulls were provided by the Missouri Crop Improvement Association (Columbia, MO). They were ground to a less than 1 mm diameter particle size and dried overnight at 70°C in a vacuum oven before use. Three samples were made with the as-received (non-ground and/or non-dried) rice hulls for comparison of the properties with the composites reinforced with the ground and dried rice hulls.

General procedure for preparation of the biocomposites

The crude resin was obtained by the mixture of 15.0 g (50 wt %) of CLO, 10.5 g (35 wt %) of BMA, and 4.5 g (15 wt %) of DVB in a beaker. Then, 1.5 g of the free-radical initiator *t*-butyl peroxide, which corresponded to an extra 5 wt % with respect to the total resin weight, was added to the monomer mixture and stirred. The rice hulls were impregnated with the crude resin and compression molded for 5 h (unless otherwise specified) at different temperatures (cure sequences I–VII, Table I). The composites were then removed from the mold and post-cured in a convection oven for 2 h at different temperatures (cure sequences I–V, Table I). As observed with the soybean hull biocomposites,[23] the filler content could not be reduced below 50 wt % because, during compression molding, the excess resin leaked out from the mold when pressure was applied. If cure was carried out at atmospheric pressure, the filler accumulated in the bottom of the mold, and a non-uniform composite was obtained. The cure temperatures, the pressure during cure, and the filler load were varied, as indicated in the text. Finally, four composites were prepared with fillers under different conditions to evaluate the effects of the drying and grinding of the rice hulls.

Characterization of the composites

Tensile tests were conducted at room temperature according to ASTM D638 with an Instron universal testing machine (Grove city, PA) (model 5569) equipped with a video extensometer and operating at a crosshead speed of 2.0 mm/min. Dogbone-shaped test specimens were machined from the original samples to give the following gauge dimensions: 57.0 × 12.7 × 4.5 mm^3 (Length × Width × Thickness, respectively). For each composite, seven dogbones were cut and tested. The results presented in the text are the average of these measurements along with the calculated standard deviation. A student's *t* test was used to confirm that each pair of results was statistically different.

DMA experiments were conducted on a Q800 DMA (TA Instruments, New Castle, DE) with the three-point bending mode with a 15.0-mm clamp. Rectangular specimens of 22.0 × 8.5 × 1.5 mm^3 (Length × Width × Thickness, respectively) were cut from the original samples. Each specimen was cooled to −60°C and then heated at 3°C/min to 250°C at a frequency of 1 Hz and an amplitude of 14 μm under air. Two runs for each sample were carried out, and the results presented in the text reflect the average of the two measurements.

A Q50 TGA instrument (TA Instruments) was used to measure the weight loss of the samples under an air atmosphere. The samples (~10 mg) were heated from room temperature to 650°C at a rate of 20°C/min.

Soxhlet extraction was conducted to determine the amount of soluble materials in the composites. A 2.0 g sample of each composite was extracted for 24 h with refluxing dichloromethane (CH_2Cl_2). After extraction, the soluble materials were recovered by the evaporation of the CH_2Cl_2 *in vacuo*. Both the soluble and insoluble materials were dried overnight at 70°C. The dried soluble fraction was then dissolved in deuterated chloroform ($CDCl_3$), and the ^{1}H-NMR spectrum was obtained with a Varian Unity spectrometer (Varian Associates, Palo Alto, CA) operating at 300 MHz. The ^{1}H-NMR spectra helped us determine the identity of the solubles in each sample.

TABLE II
Tensile Test, DMA, TGA, and Soxhlet Extraction Results for Composites Cured Under 400 psi and Different Temperatures and Times

Cure sequence	E (GPa)	Tensile strength (MPa)	T_g (°C)	E' at 130°C (MPa)	T_{10} (°C)	Residue (wt %)	Soluble fraction (wt %)[d]
I	0.8 ± 0.1	2.4 ± 0.4	26	102	289	15	6
I[a]	0.7 ± 0.1	3.2 ± 0.3	25	98	290	15	6
II	1.2 ± 0.1	3.7 ± 0.3	30, 73[b]	137	294	14	6
III	1.4 ± 0.4	5.4 ± 0.8	43	209	291	14	6
IV	1.8 ± 0.1	6.7 ± 0.7	68	336	304	14	5
V	1.7 ± 0.1	5.8 ± 2.7	66	149	352	21	4
VI	1.0 ± 0.5	0.7 ± 0.5	59	45	297	14	14
VII	1.1 ± 0.4	0.8 ± 0.3	—[c]	—[c]	298	14	13

[a] Composite made under the same conditions but from a different batch.
[b] Two distinct T_g's were observed (30 and 73°C).
[c] The sample submitted to cure sequence VII tended to crumble very easily when handled; therefore, DMA specimens could not be machined for the determination of Tg and E' at 130°C.
[d] Determined by Soxhlet extraction.

DSC experiments were performed on a Q20 DSC instrument (TA Instruments) under an N_2 atmosphere over a temperature range of −20 to 400°C at a heating rate of 20°C/min. The samples weighed about 10 mg.

For the SEM analysis, each sample was frozen with liquid nitrogen before fracturing (cryofracturing). A second section of the sample was mechanically cut and shaved with a razor blade to provide a smooth cross section. Both cryofractured and cut samples were examined with a Hitachi S-2460N (Tokyo, JAPAN) variable-pressure scanning electron microscope. The microscope was operated at a 20-kV accelerating voltage, with 60 Pa of a helium atmosphere, and a 25-mm working distance. Backscattered electron images were collected with a Tetra BSE detector (Concord, MA) (Oxford Instruments) at 35 and 100× magnifications. An Oxford ISIS X-ray analyzer (Concord, MA) with a light-element detector was used to collect an X-ray map of a section of the cut surface at a 200× magnification.

RESULTS AND DISCUSSION

Cure sequence study

To determine the optimum cure sequence, seven samples bearing the same resin composition and filler load (70 wt %) were exposed to different temperatures, as shown in Table I. The cured composites were then analyzed by tensile tests, DMA, TGA, and Soxhlet extraction. The results are presented in Table II.

For an assessment of the reproducibility of the composites' properties, cure sequence I was applied to composites from different batches under otherwise identical conditions (cure sequence I[a], Table II). The results show an overall agreement between the properties measured for the two samples, especially when the differences between the properties obtained for cure sequences I and I[a] were compared to the variations observed for the other cure sequences used (cure sequences II–VII, Table I).

From the tensile test results, there was an overall increase in both the Young's modulus and the tensile strength when the cure temperature was increased from 130°C to 180°C (cure sequences I–IV, Table II). A significant drop in the tensile strength was observed when the composite was cured at 230°C (cure sequence V, Table II). In that case, the exceedingly high cure temperature used in cure sequence V initiated thermal degradation of the rice hulls and affected the tensile properties of the final composite. The absence of a post-cure step during cure sequences VI and VII had a dramatic effect on the tensile properties of the composites, independent of the duration of cure. The Young's modulus decreased to around 1.0 GPa for the composites cured at 180°C for 5 h and 7 h (cure sequences VI and VII, Table II). A more pronounced decrease was observed in the tensile strength of these composites (cf. cure sequences VI and VII with cure sequence IV, Table II). This indicated that the post-cure was a key step during the preparation of the biocomposites. It helped to maximize the mechanical properties through an increase in the crosslink density and full incorporation of all of the comonomers used in the synthesis.

The glass-transition temperatures (T_g's) were determined from the tan δ curves obtained by DMA. Similar to the Young's modulus and the tensile strength, an increase in T_g for the composites was seen with increasing cure temperatures. T_g increased from 26°C to 68°C when the cure temperature was increased from 130°C to 180°C (cure sequences I–IV, Table II). This increase in T_g may have indicated a higher degree of cure obtained when higher temperatures were used during processing. At lower temperatures, the polymerization rate was low, and the product obtained

after the process was not fully cured. As the cure temperature was increased, a higher polymerization rate yielded a higher degree of cure; this increased the final T_g as a consequence. The occurrence of a second T_g for cure sequence II was not completely understood. In some of our previous work,[23] the appearance of two T_g's was observed when a resin containing comonomers with distinctly different reactivities (e.g., conjugated soybean oil, BMA, and DVB) was cured under high pressures and high filler loads, but here, these parameters were kept constant. When the cure temperature was increased to 230°C (cure sequence V, Table II), a slight decrease in T_g was observed. The absence of a post-cure step (cure sequence VI, Table II) resulted in a composite that was only partially cured. The composite cured under cure sequence VII crumbled too easily when handled to be analyzed by DMA.

The storage modulus (E') of the biocomposites was determined at 130°C, significantly above the T_g, where a better relationship could be established between the parameters changed and E' of the composites analyzed. Overall, the results followed the same trend observed for the tensile properties. An increase in E' was seen with increasing cure temperatures. A significant drop in E' was observed when cure sequences IV and V were compared (see Table II), and a dramatic decrease in E' was detected when no post-cure was applied (cure sequence VI, Table II). These results suggest that the post-cure was essential for obtaining a fully cured composite, and cure sequence IV seemed to be optimal for this system.

T_{10} represents the temperature at 10 wt % degradation of the composites, as determined by TGA. This temperature occurred between 289°C and 352°C for all of the composites included in Table II. There was an overall increase in this value with increasing cure temperature (cure sequences I–V, Table II). However, the small differences observed between cure sequences I, II, and III were insignificant when the overall trend was considered and may have been due to experimental variation. As mentioned before, with higher cure temperatures, partial degradation of the less stable filler components (e.g., hemicellulose) increased during cure. Indeed, reports indicate that hemicellulose starts to degrade at temperatures as low as 175°C.[27] During TGA of those partially degraded materials (cure sequences IV–VII), a higher temperature was required to attain T_{10} because the composite had a higher content of more stable components. The T_{10} values of samples that were not post-cured (cure sequences VI and VII, Table II) were slightly lower than the T_{10} of the composite cured under cure sequence IV (Table II). This indicated that the 2 h post-cure at 200°C (cure sequence IV, Table I) was probably responsible for the partial degradation of the filler. Furthermore, the rice hulls alone exhibited a T_{10} of 286°C (result not shown in Table II), which implied that temperatures lower than T_{10} for the composites may have already started degrading the filler.

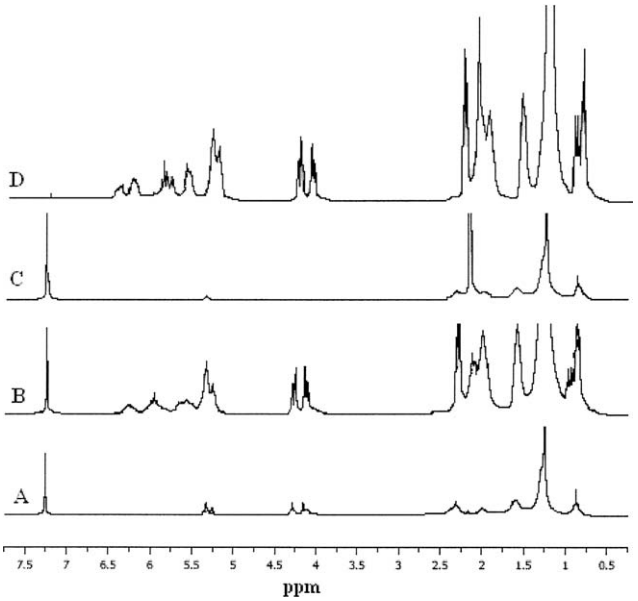

Figure 1 ^{1}H-NMR spectra of (A) extract of the composite cured under cure sequence IV, (B) extract of the composite cured under cure sequence VII, (C) extract of the rice hulls, and (D) CLO.

With the exception of three entries in Table II, the residue left after 650°C during the TGA corresponded to 14 wt %. For reasons expressed earlier, the composite cured under cure sequence V had a higher residue content. Presumably, the higher temperature used during cure degraded the less stable filler components to a greater extent and left a higher concentration of minerals and more stable structures in the composite. The slightly higher residue content found for the sample cured with cure sequence I may have been due to experimental variation during the weighing of the filler and resin for preparation of the composite. The residue was rich in silica, as confirmed later during X-ray mapping analysis and as reported in the literature for rice straw.[28]

Finally, most of the composites afforded 4–6 wt % soluble materials after cure (cure sequences I–V, Table II). This indicated that the majority of the resin components were incorporated into the resin during cure and that a high crosslink density was attained. In the two cure sequences where a post-cure step was not used (cure sequences VI and VII, Table II), a much larger soluble content was found. From the ^{1}H-NMR spectra of the extracts, we observed clearly that the soluble content recovered from the composites [Fig. 1(A,B)] resembled the unreacted CLO [Fig. 1(D)]. The intensity of the peaks in Figure 1(A) was much lower than that of Figure 1(B,D) because

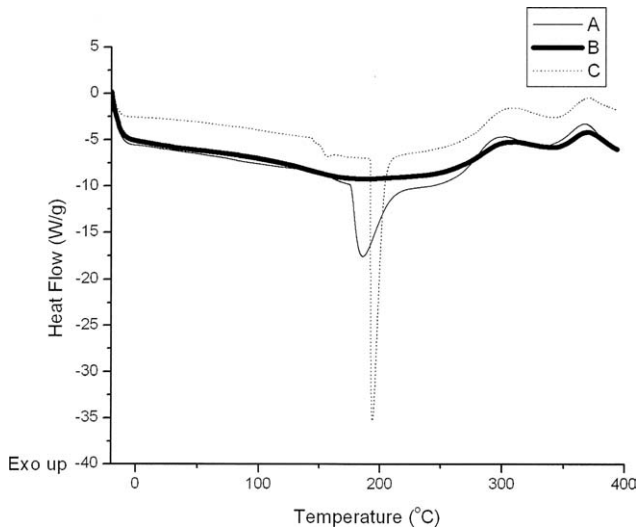

Figure 2 DSC curves of (A) the composite cured under cure sequence VII, (B) the composite cured under cure sequence IV, and (C) rice hulls.

of the low amount of soluble materials recovered, but the presence of the methylene hydrogen peaks between 4.0 and 4.5 ppm confirmed the presence of a triglyceride unit in the extract. Also worth mentioning is the fact that the rice hulls alone exhibited a soluble content of 10 wt % (result not shown in Table II) which consisted of an oily material rich in hydrocarbon residues, as illustrated by the peaks between 0.5 and 2.5 ppm in the ^{1}H-NMR spectrum [Fig. 1(C)], corresponding to hydrogens attached to sp^3 hybridized carbons.

A comparison of the DSC curves of rice hulls and composites cured under different cure sequences is provided in Figure 2. The most distinctive feature of these curves is the endothermic peak that occurred at 194°C for the rice hulls [Fig. 2(C)]. This peak was attributed to the volatilization of compounds formed during the degradation of the hemicellulose[29] and matched the beginning of the second weight loss step observed in the TGA curve (figure not shown). The rice hulls also exhibited a change in the baseline at 152°C that is not presently understood. In the composite undergoing cure sequence VII [Fig. 2(A)], the endothermic peak was less intense and shifted to a lower temperature (190°C). This phenomenon could have been related to partial degradation of the hemicellulose during the cure process. Indeed, during thermal degradation, the hemicellulose chain was broken down to smaller structures that required lower temperatures to volatilize. Also, because some components had already volatilized during cure, the intensity of the peak was noticeably lower. For the composite cured under cure sequence IV [Fig. 2(B)], the endothermic peak completely disappeared, and no transitions were observed between 0°C and 250°C; this indicated that the resin was fully cured and that the composite was completely stable in that temperature range. The transitions occurring after 250°C were attributed to the thermal degradation of the samples and are not individually analyzed here.

Given the results presented so far, cure sequence IV yielded a fully cured resin and a composite with the best mechanical properties among those prepared as discussed in this section. Therefore, cure sequence IV was used in the preparation of all of the composites discussed in the remainder of this article.

Influence of the pressure during cure on the properties of the rice hull biocomposites

The variation of the cure pressure during the preparation of the composites had an impact on the final properties obtained, as shown in Table III. Young's modulus increased when the pressure increased from 276 psi to 600 psi. In this case, we observed an increase in E, by a purely mechanical action. The increase in pressure minimized the presence of microvoids in the final composites and, therefore, improved the modulus. For the tensile strength, there was a decrease when the pressure was increased from 400 psi to 600 psi (Table III). Lower tensile strengths indicated that the composites were less tolerant to deformations, and they became more brittle when higher pressures were used during cure. When a very low pressure (276 psi) was used in the preparation of the composite, the presence of

TABLE III
Tensile Tests, DMA, TGA, and Soxhlet Extraction Results for Rice Hull Composites Containing 70 wt % Rice Hulls Cured Under Various Pressures with Cure Sequence IV

Pressure (psi)	E (GPa)	Tensile strength (MPa)	T_g (°C)	E' at 130°C (MPa)	T_{10} (°C)	Residue (wt %)	Soluble fraction (wt %)[a]
276	1.6 ± 0.3	5.5 ± 1.2	66	37	309	15	6
400	1.8 ± 0.1	6.7 ± 0.7	68	336	304	14	5
500	2.0 ± 0.3	6.2 ± 0.8	69	417	306	15	6
600	2.3 ± 0.5	5.9 ± 0.6	52	220	304	15	5

[a] Determined by Soxhlet extraction.

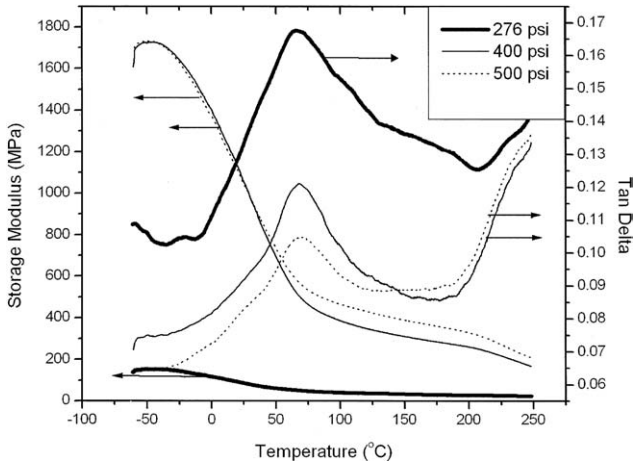

Figure 3 E' and tan δ curves for samples cured under 276 psi, 400 psi, and 500 psi. The composites had 70 wt % ground filler and were cured under a specified pressure with cure sequence IV.

microvoids was so significant that even the tensile strength of the material was compromised.

A slight increase in T_g was observed with increasing pressure from 276 psi to 500 psi (Table III), but because of the very low variability of T_g in that pressure range, it was difficult to establish a relationship between the cure pressure and T_g of the composites, as shown in Figure 3. Nevertheless, the composite cured under 600 psi exhibited a T_g of 52°C. This constituted a significant decrease from the T_g of the composite cured at 500 psi. In one of our previous studies,[23] we demonstrated that the cure pressure could affect the polymerization of the resin. Here, we assumed that the high pressure affected the mobility and dispersion of the resin comonomers through the filler particles during polymerization, and as a consequence, a matrix with a lower T_g was obtained. The E' values followed the same trends observed for the T_g's, with an increase when the cure pressure increased from 276 psi to 500 psi (Table III, Fig. 3), and a significant decrease was observed in the modulus when the pressure increased from 500 psi to 600 psi. The remarkably low modulus obtained with a 276 psi cure pressure (Fig. 3) was attributed to poor filler–resin interaction, which compromised the stress transfer from the matrix to the filler.

The T_{10} values, residue and soluble fraction changed very little when different cure pressures were used during preparation of the composites. The T_{10} value and the residue were closely related to the resin and material composition, whereas the soluble fraction was an indirect measurement of the crosslink density of the matrix. Because the filler material and resin composition were kept constant throughout this study, no significant changes were expected for the thermal degradation profile of the composites, and a soluble content of approximately 5 wt % was expected for any composite cured under cure sequence IV (Table II).

Because the aim of this study was to produce a rigid composite with good mechanical properties for the possible replacement of petroleum-derived polymers, the cure pressure that gave the stiffest material (600 psi) was chosen for use in the remainder of this study.

Influence of the filler load on the properties of the rice hull biocomposites

Table IV shows the effect of the filler load on the composite properties. There was an increase in the Young's modulus, tensile strength, and E' when the filler load was increased from 50 wt % to 70 wt %. The increase in the mechanical properties revealed the reinforcement behavior of the rice hulls in the composite in a filler load range where there was enough resin to wet all of the filler particles. This reinforcing behavior of the rice hulls was also observed when we compared E' of an unreinforced conjugated soybean oil-based resin and any of the composites shown in Table IV. Indeed, a significant increase was observed whenever rice hulls were present. Beyond 70 wt % filler load, a decrease in the tensile properties was observed. This drop in

TABLE IV
Tensile Tests, DMA, TGA, and Soxhlet Extraction Results for Rice Hull Biocomposites Prepared Under Cure Sequence IV and 600 psi with Various Filler Loads

Filler load (wt %)	E (GPa)	Tensile strength (MPa)	T_g (°C)	E' at 130°C (MPa)	T_{10} (°C)	Residue (wt %)	Soluble fraction (wt %)[c]
—[a]	—	—	−51, 37[b]	44	344	0	13
50	0.6 ± 0.2	1.1 ± 0.8	32	82	308	9	7
60	1.4 ± 0.4	4.7 ± 1.6	63	172	302	10	5
70	2.3 ± 0.5	5.9 ± 0.6	52	220	304	15	5
80	1.7 ± 0.8	2.6 ± 1.6	−18, 93[b]	83	294	12	5
90	0.9 ± 0.5	0.6 ± 0.5	−29, 66[b]	87	292	13	4

[a] Unreinforced resin containing 50 wt % conjugated soybean oil, 35 wt % BMA, and 15 wt % DVB.[23]
[b] Two distinct T_g's were observed.
[c] Determined by Soxhlet extraction.

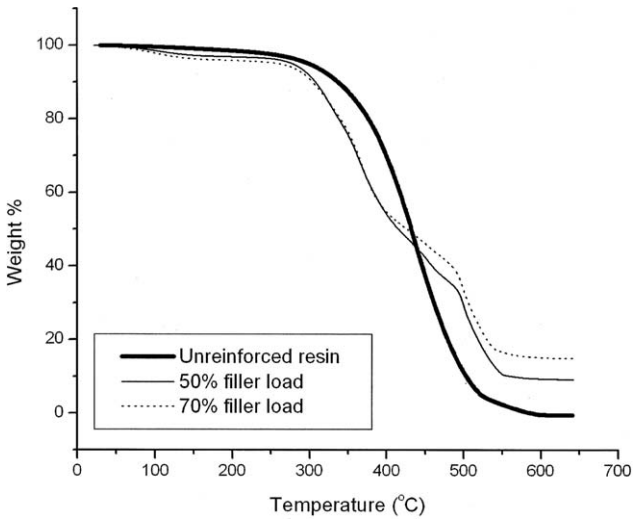

Figure 4 TGA curves for a soybean oil-based unreinforced resin and composites containing 50 wt % and 70 wt % rice hulls. The resin composition was 50 wt % conjugated vegetable oil, 35 wt % BMA, and 15 wt % DVB.

the tensile properties was attributed to a lack of resin to bind all of the filler particles efficiently, and it resulted in an agglomeration of the filler and weak points in the composite structure that were responsible for the lower performance of the material. The same phenomenon was observed previously with soybean hull composites.[23] As for E', there was a significant decrease above 70 wt % filler load (Table IV) for reasons mentioned previously. The variation in E' for samples containing 80 wt % and 90 wt % filler was negligible when compared to the drop observed between 70 wt % and 80 wt %.

Between 50 wt % and 70 wt % filler load, no regular pattern in the T_g values could be distinguished (Table IV). However, two T_g's were observed when the filler load was 80 wt % and 90 wt % (Table IV). In these instances, the high filler load may have compromised the dispersion of the different comonomers throughout the system and affected the chain growth during polymerization. For the unreinforced conjugated soybean oil-based resin, a difference in the reactivity of the comonomers promoted a phase separation of the resin. Indeed, a phase separation of vegetable oil-based resin has been previously observed,[10,22,23] and it is believed that the two phases formed consisted of a vegetable oil-rich phase and a DVB-rich phase.

The T_{10} values did not vary much for filler contents varying between 50 wt % and 70 wt %, and no specific trend was observed (Table IV). There was a 10°C drop in T_{10} for 80 wt % and 90 wt % filler loads with respect to the 70 wt % and 60 wt % composites, respectively. As mentioned before, the T_{10} value of the rice hulls alone (286°C) was lower than that of the resin (344°C). So in systems where the rice hulls were in a large excess (80 wt % and beyond), it was normal to observe a decrease in T_{10}. The percentage residue increased when the filler load was increased from 50 wt % to 70 wt % (Table IV). The rice hulls alone exhibited a residue content of 18 wt % (result not shown in Table IV), whereas the unreinforced resin left no residue. This indicated that the majority of the residue left after thermal degradation came from the reinforcement. Therefore, we expected that an increase in the filler content would produce an increase in the residue after degradation. This trend was not observed for the samples containing 80 wt % and 90 wt % filler, which exhibited essentially the same residue, with a negligible difference.

Figure 4 provides a comparison of the thermal degradation patterns of the unreinforced resin and samples containing 50 wt % and 70 wt % rice hulls. From this comparison, a few key features from the degradation of the filler stood out, such as the loss of water between 100° and 150°C and the two distinct degradation steps before and after 450°C, which were related to the cellulose/lignin composition of the filler. There was also a noticeable increase in the residue percentage with filler content.

There was not a significant variation in the soluble fraction recovered from the composites with different filler loads. The values ranged from 4 wt % to 7 wt % soluble materials (Table IV). With such a small variation, it was impossible to establish a reliable relationship between the filler content and the amount of soluble materials recovered after Soxhlet extraction. The unreinforced resin, on the other hand, exhibited 13 wt % soluble materials, consisting mainly of unreacted oil. These results suggest that the resin was the main source of soluble content in the composites; this corroborated the results shown in Figure 1.

As stated before, the goal of this study was to find a rice hull biocomposite with the best mechanical properties possible. Given the results presented in Table IV, a filler load of 70 wt % gave the best overall properties and was, therefore, used to study the influence of the drying and grinding of the filler on the final properties of the composite.

Influence of the drying and grinding of the filler on the properties of the rice hull biocomposites

Table V summarizes the properties obtained for four composites prepared under the same conditions, differing only with respect to the conditions of the rice hulls used as the fillers. The rice hulls used were (1) as received, (2) dried but not ground, (3) non-dried but ground, and (4) dried and ground.

The mechanical properties of these biocomposites revealed a great improvement in the composite's performance whenever the rice hulls were dried before

TABLE V
Tensile Tests, DMA, TGA, and Soxhlet Extraction Results for Rice Hull Biocomposites Prepared Under Cure Sequence IV and 600 psi Containing 70 wt % of Various Rice Hull Fillers

Rice hulls	E (GPa)	Tensile strength (MPa)	T_g (°C)	E' at 130°C (MPa)	T_{10} (°C)	Residue (wt %)	Soluble fraction (wt %)[a]
As received	0.7 ± 0.4	1.4 ± 0.8	40	21	297	16	6
Dried, non-ground	2.3 ± 0.4	5.7 ± 0.6	41	280	303	16	5
Non-dried, ground	1.0 ± 0.3	1.7 ± 1.0	58	199	298	17	5
Dried, ground	2.3 ± 0.5	5.9 ± 0.6	52	220	304	15	5

[a] Determined by Soxhlet extraction.

use. Indeed, the Young's modulus increased when the whole rice hulls were dried before they were impregnated with the resin (Table V). Similarly, there was an increase in the Young's modulus when the ground rice hulls were dried (Table V). The tensile strength of the composites showed the same trend, with increases when the whole and the ground rice hulls were dried (Table V). Along the same lines, E' at 130°C increased when dried versus non-dried whole rice hulls were used and also increased when the ground rice hulls were dried before use. This increase in the mechanical properties was probably related to the fact that the lower moisture content in the dried rice hulls may have led to a better filler–resin interaction, which gave better stress transfer from the matrix to the reinforcement and, consequently, better tensile properties.

The grinding of the rice hulls had little effect on the tensile properties of the composites in comparison to the variations observed between the dried and non-dried fillers. The slight increase in the Young's modulus observed when non-dried whole rice hulls and ground rice hulls were compared could be neglected because it fell within the standard deviations of the corresponding samples (Table V). Also, virtually no change was observed when the dried rice hulls were compared (Table V). The same happened with the tensile strength; increases within the standard deviation of the samples were observed for non-dried whole and ground rice hulls and for dried whole and ground rice hulls (Table V). The better tensile properties normally obtained for composites with smaller particle sizes were compensated for here by a loss in the aspect ratio of the non-ground rice hulls. Therefore, grinding the rice hulls meant going from an elongated structure with better tensile properties but a lower dispersion in the matrix to more spherical particles, which dispersed better in the matrix but showed lower tensile properties.

For E' at 130°C, drying the rice hulls had a similar effect to that observed on the tensile properties. A significant increase occurred when the whole rice hulls were dried (Table V). A more subtle increase was observed between non-dried and dried ground rice hulls (Table V). The effect on E' at 130°C of grinding the rice hulls was unclear, as opposite trends were observed for the dried and non-dried fillers. An increase was observed when the whole and ground non-dried rice hulls were compared, whereas a decrease was observed when the whole and ground dried rice hulls were compared (Table V). T_g, on the other hand, appeared to be more sensitive to variations in the filler particle size. Indeed, grinding the rice hulls increased T_g of the composite by at least 11°C (Table V). This effect was observed previously with soybean hull composites[23] and was attributed to a better mix of resin and filler when smaller particle sizes were used. Very little effect was observed when the T_g's of the non-dried and dried whole rice hulls were compared or when non-dried and dried ground rice hulls were compared (Table V).

The T_{10} values were only slightly changed when the dried and non-dried rice hulls were compared. The slight differences observed between the T_{10} values of the non-dried and dried whole rice hulls and of the non-dried and dried ground rice hulls were due to the moisture content of the filler. When the filler was dried before use, it lost approximately 7 wt % because of moisture (result not shown in Table V). For the composites reinforced with non-dried rice hulls, T_{10} reflected the loss of that moisture content from the filler, along with the partial volatilization of some resin components, and as the moisture should have been completely lost around 100°C, the T_{10} value of those materials shifted slightly to lower temperatures. From the negligible difference observed between the T_{10} values of the non-ground and ground dried hulls and non-ground and ground non-dried hulls (Table V), we concluded that grinding the rice hulls had no effect on the T_{10} values of the composites.

Finally, there was virtually no variation in the residue content and soluble content extracted when the rice hulls were dried and/or ground (Table V). As mentioned before, those properties were related to the amount of filler and the composition of the resin used in the preparation of the composites, and because those parameters were kept constant for all of the samples shown in Table V, no variation was expected here.

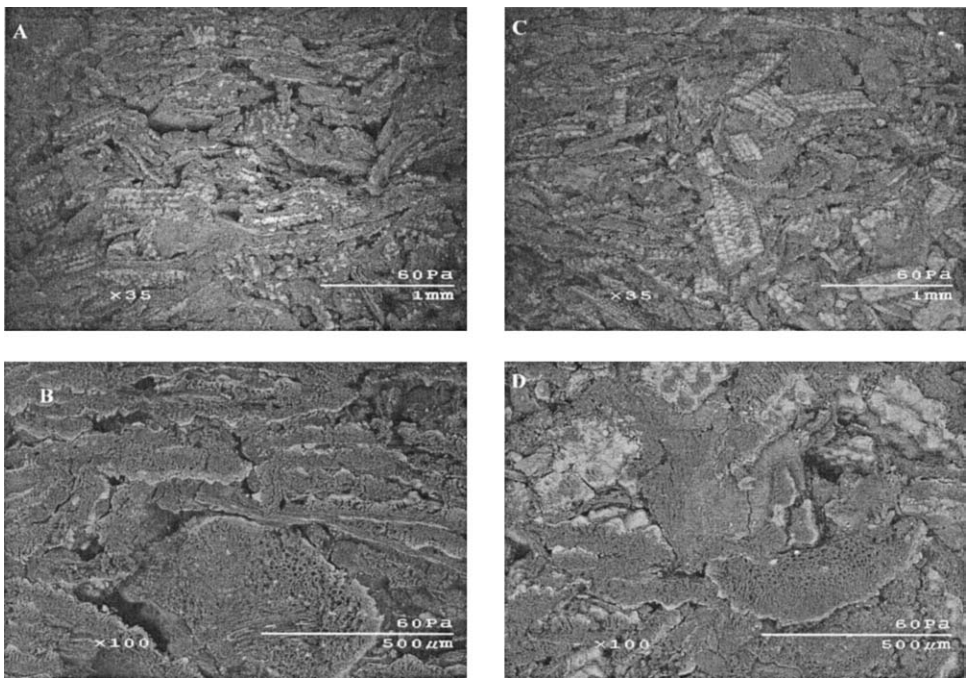

Figure 5 SEM images of (A) the cryofractured biocomposite reinforced with dried rice hulls (35× magnification), (B) the cut biocomposite reinforced with dried rice hulls (100× magnification), (C) the cryofractured biocomposite reinforced with non-dried rice hulls (35× magnification), and (D) the cut biocomposite reinforced with non-dried rice hulls (100× magnification). Both composites had 70 wt % ground filler and were cured under 600 psi at 180°C for 5 h and then post-cured at ambient pressure for 2 h at 200°C.

SEM analysis of the rice hull biocomposites

Figure 5 depicts the SEM images of the cryofractured and cut biocomposite samples. Samples made with dried and non-dried rice hulls were analyzed and compared. Both composites had a filler load of 70 wt % and were cured under 600 psi at 180°C for 5 h and then post-cured at ambient pressure for 2 h at 200°C.

From the SEM of the composites (Fig. 5), it was possible to clearly identify the rice hull particles intercalated with the resin. The brighter regions on the images represent the structures of higher density, located mostly on the surface of the rice hulls. Those structures are discussed further later in the text. The porous structures observed, for example, in Figure 5(B), corresponded to rice hull particles. As expected, the large amount of rice hulls used (70 wt %) resulted in composites where the resin was present in minimal amounts and functioned mainly as a binder between the rice hull particles. Significant voids were observed in all four images, which indicated the overall bad interaction between the filler and the resin. The presence of voids also indicated weak regions in the composites, where cracks could be easily generated and/or propagated.

The images of the cryofractured composites [Fig. 5(A,C)] showed a more significant exposition of the silica structures; this again indicated poor resin–filler adhesion. When the samples were fractured, the crack propagated along the resin–filler interface; this left the rice hull particle surfaces exposed. Comparatively more of the silica structures are shown in Figure 5(C), where non-dried rice hulls were used. This is an indication that worse resin–filler interactions were obtained when non-dried filler particles were used because of the incompatibility of the hydrophobic resin and the hydrophilic filler. Furthermore, Figure 5(A) shows more resin artifacts covering the rice hull particles.

Figure 5(B,D) shows, in more detail, the filler–resin interface. The central area in Figure 5(B) shows a region where the resin and filler interacted well (there was no discontinuity between the matrix and the reinforcement). Nothing similar was observed in the entirety of Figure 5(D); this supported the idea that worse filler–resin interactions were present when the fillers were not dried before their use as a reinforcement in the manufacturing of the biocomposites.

X-ray map of a rice hull biocomposite sample

An X-ray map of a rice hull biocomposite sample cured at 600 psi under cure sequence IV is shown in Figure 6. Figure 6(A) shows the SEM image of the cut biocomposite at 200× magnification. From that image, it is clear that the denser region (brighter areas) was more abundant on the surface of the rice hull particles. The presence of significant amounts of

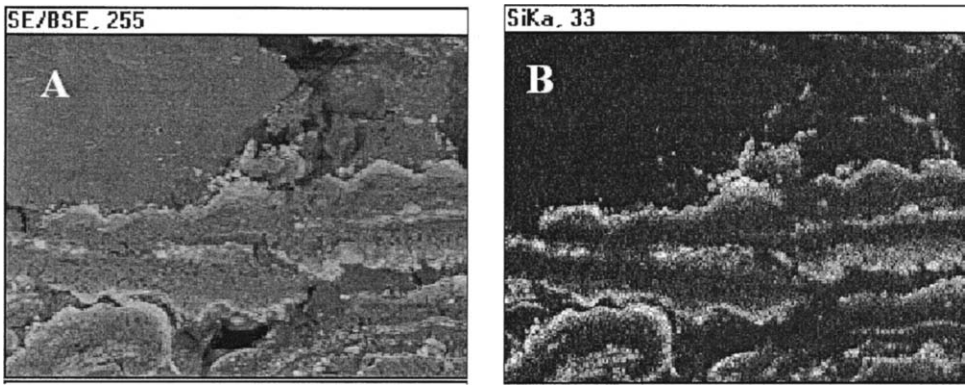

Figure 6 (A) SEM image of the biocomposite with 70 wt % ground filler cured under 600 psi at 180°C for 5 h and then post-cured at ambient pressure for 2 h at 200°C and (B) X-ray map of line Si Ka on the same section shown in part A.

silica in rice straw ash suggested that these high-density structures were most likely SiO_2.[28]

Figure 6(B) shows the Si X-ray map of the same composite shows in figure 6(A). When Figures 6(A) and 6(B) were compared, it became clear that the rice hulls were rich in Si and that the Si-containing structures were more abundant on the surface of the rice hulls. The presence of silica in the rice hulls explained the high mechanical properties obtained for the biocomposites prepared in this study.

CONCLUSIONS

Rice hull biocomposites were prepared by the free-radical polymerization of a CLO-based resin. After the cure study, an optimal cure sequence of 5 h at 180°C under pressure followed by 2 h of post-cure under ambient pressure was established. The mechanical data, along with TGA, Soxhlet extraction, and DSC results, showed that the post-cure step was crucial for obtaining a fully cured resin, and the best CLO incorporation in the matrix. The effects of pressure during cure, filler load, and drying and grinding of the filler on the final properties of the biocomposites were assessed, and optimal conditions were established for the preparation of the rice hull-reinforced composites. A pressure of 600 psi during the cure resulted in the stiffest material. The use of 70 wt % dried and ground (<1 mm diameter particle size) filler afforded the best overall properties. SEM showed evidence of weak filler–resin interactions due to differences in the hydrophilicity of the matrix and the reinforcement. The SEM analysis also provided an indication of a denser material present on the surface of the rice hulls. The Si X-ray map indicated a high Si content in that material, which consisted, most likely, of silica. The presence of significant amounts of silica in the rice hulls may have accounted for the high thermal stability and the high mechanical properties obtained for the rice hull biocomposites. A thorough resin composition study is currently being carried out and will soon be reported.

The authors thank the Missouri Crop Improvement Association for the rice hulls, Michael Kessler from the Department of Material Sciences and Engineering and Richard Hall from the Department of Natural Resource Ecology and Management at Iowa State University for the use of their facilities, Warren Straszheim from the Department of Material Sciences and Engineering for help with the SEM and X-ray mapping experiments, and Douglas Stokke from the Department of Natural Resource Ecology and Management for important information concerning the rice hulls.

References

1. Lu, Y.; Larock, R. C. Biomacromolecules 2007, 8, 3108.
2. Lu, Y.; Larock, R. C. Biomacromolecules 2008, 9, 3332.
3. Andjelkovic, D. D.; Larock, R. C. Biomacromolecules 2006, 7, 927.
4. Andjelkovic, D. D.; Lu, Y.; Kessler, M. R.; Larock, R. C. Macromol Mater Eng 2009, 294, 472.
5. Jeong, W.; Mauldin, T. C.; Larock, R. C.; Kessler, M. R. Macromol Mater Eng 2009, 294, 756.
6. Valverde, M.; Andjelkovic, D.; Kundu, P. P.; Larock, R. C. J Appl Polym Sci 2008, 107, 423.
7. Li, F.; Hasjim, J.; Larock, R. C. J Appl Polym Sci 2003, 90, 1830.
8. Li, F.; Larock, R. C. Biomacromolecules 2003, 4, 1018.
9. Henna, P. H.; Andjelkovic, D. D.; Kundu, P. P.; Larock, R. C. J Appl Polym Sci 2007, 104, 979.
10. Andjelkovic, D. D.; Valverde, M.; Henna, P.; Li, F.; Larock, R. C. Polymer 2005, 46, 9674.
11. Jarukumjorn, K.; Suppakarn, N. Compos B 2009, 40, 623.
12. Srebrenkoska, V.; Gaceva, G. B.; Dimeski, D. Maced J Chem Chem Eng 2009, 28, 99.
13. Haque, M. M.; Hasan, M.; Islam, M. S.; Ali, M. E. Bioresour Technol 2009, 100, 4903.
14. Panthapulakkal, S.; Zereshkian, A.; Sain, M. Bioresour Technol 2006, 97, 265.
15. Sui, G.; Fuqua, M. A.; Ulven, A. A.; Zhong, W. H. Bioresour Technol 2009, 100, 1246.
16. Vilaseca, F.; Valady-Gonzalez, A.; Herrera-Franco, P. J.; Pelach, M. A.; Lopez, J. P.; Mutje, P. Bioresour Technol 2010, 101, 387.

17. Liu, H.; Wu, Q.; Zhang, Q. Bioresour Technol 2009, 100, 6088.
18. Xu, Y.; Wu, Q.; Lei, Y.; Yao, F. Bioresour Technol 2010, 101, 3280.
19. Onal, L.; Karaduman, Y. J. Comp Mater 2009, 43, 1751.
20. Hapuarachchi, T. D.; Ren, G.; Fan, M.; Hogg, P. J.; Peijs, T. Appl Compos Mater 2007, 14, 251.
21. Reddy, N.; Yang, Y. J Appl Polym Sci 2010, 116, 3668.
22. Pfister, D. P.; Larock, R. C. Bioresour Technol 2010, 101, 6200.
23. Quirino, R. L.; Larock, R. C. J Appl Polym Sci 2009, 112, 2033.
24. Bhuyan, S.; Sundararajan, S.; Pfister, D.; Larock, R. C. Tribol Int 2010, 43, 171.
25. Pfister, D. P.; Baker, J. R.; Henna, P. H.; Lu, Y.; Larock, R. C. J Appl Polym Sci 2008, 108, 3618.
26. Larock, R. C.; Dong, X.; Chung, S.; Reddy, C. K.; Ehlers, L. E. J Am Oil Chem Soc 2001, 78, 447.
27. Barneto, A. G.; Carmona, J. A.; Alfonso, J. E. M.; Alcaide, L. J. Bioresour Technol 2009, 100, 3963.
28. Abdel-Mohdy, F. A.; Abdel-Halim, E. S.; Abu-Ayana, Y. M.; El-Sawy, S. M. Carbohydr Polym 2009, 75, 44.
29. Yang, H.; Yan, R.; Chen, H.; Lee, D. H.; Zheng, C. Fuel 2007, 86, 1781.